Raman scattering from ion-implanted graphite

B. S. Elman
Center for Materials Science and Engineering and the Department of Physics, Massachusetts Institute of Technology, Cambridge, Massachusetts 02139

M. S. Dresselhaus
Center for Materials Science and Engineering and the Department of Electrical Engineering and Computer Science, Massachusetts Institute of Technology, Cambridge, Massachusetts 02139

G. Dresselhaus
Francis Bitter National Magnet Laboratory, Massachusetts Institute of Technology, Cambridge, Massachusetts 02139

E. W. Maby
Center for Materials Science and Engineering and the Department of Electrical Engineering and Computer Science, Massachusetts Institute of Technology, Cambridge, Massachusetts 02139

H. Mazurek
Center for Materials Science and Engineering, Massachusetts Institute of Technology, Cambridge, Massachusetts 02139
(Received 8 December 1980)

Ion-implanted graphite is studied by Raman scattering. Highly oriented pyrolytic graphite is implanted with ^{7}Li, ^{9}Be, ^{11}B, ^{12}C, ^{31}P, and ^{75}As ions at 100 keV normally incident upon the c face. Ion fluences in the range 1×10^{14} to 2.5×10^{16} ions/cm^2 are used. The lattice damage upon implantation is monitored by observation of the disorder-induced Raman line at ~ 1355 cm^{-1} in the first-order spectra and at ~ 2970 cm^{-1} in the second-order spectra. The Raman results indicate that an abrupt transformation to an amorphous surface layer occurs at a critical fluence which varies with the mass of the implanted ion. Results for first- and second-order Raman spectra are also presented for the same ion-implanted samples upon isochronal vacuum annealing at various annealing temperatures, showing a partial restoration of the graphite ordering. The second-order Raman spectra are even more sensitive than the first-order spectra to the creation of lattice damage by ion implantation and to the subsequent partial restoration of lattice order by annealing.

INTRODUCTION

Intercalation has been widely used as a mechanism for chemical introduction of foreign species into layered host materials such as graphite. Graphite intercalation compounds are interesting because of the large varieties of behavior that can be produced by intercalation, such as the occurrence of superconductivity in C_8K, where neither C nor K are superconducting, the increases by nearly two orders of magnitude in the in-plane conductivity σ_a and the increase by more than two orders of magnitude in the electrical anisotropy ratio σ_a/σ_c where σ_c is the c-axis conductivity.

Ion implantation provides a physical mechanism for the introduction of foreign species into these host materials, making possible the introduction of species that do not intercalate by chemical means. Because of the high kinetic energy of insertion, it may be possible to create more stable materials with lower affinities for desorption of the guest species. This kinetic energy, however, introduces lattice disorder which affects various physical properties of these materials. Therefore the lattice damage must

be monitored.

As an implanted ion (typically of ~ 100 keV energy) slows down and comes to rest, it makes many violent collisions with lattice atoms, displacing them from their lattice sites. Some of these displaced atoms have enough kinetic energy to displace others, giving rise to a cascade process. The net result is the production of a highly disordered region around the path of the ion with the dominant disorder occurring near the end of the ion trajectory, as shown schematically in Fig. 1(a). At sufficiently high dosage, these individual disordered regions begin to overlap [Fig. 1(b)] until finally a noncrystalline or amorphous layer is formed [Fig. 1(c)]. Such a mechanism for the introduction of disorder is well known from studies of Si and Ge.[1]

The method of ion implantation in fact provides a technique for artificially producing disordered regions of varying sizes [Fig. 1(b)] by appropriate selection of the dose of implanted ions. Ion implantation allows study of the evolution of the microscopic structural properties of a very important sequence of regimes: crystalline-microcrystalline-amorphous.

This paper focuses on the use of Raman scattering as a tool to monitor the ion-implantation process in graphite. Since ion implantation takes place within an optical skin depth, Raman scattering which probes the sample within an optical skin depth provides a sensitive tool for monitoring the implantation process. Raman scattering has in fact been widely exploited to characterize ion-implanted silicon[2–4] and to some extent also graphite.[2,5–7] Since graphite is a crystalline material, the profile and range of the ion-induced disorder is sensitive to the angle of ion incidence to the layer planes, so that control of the disorder generation is more difficult than for amorphous or glassy substrates. The first- and second-order Raman spectra reported here for boron-implanted graphite provide evidence for the three regimes of behavior delineated above.

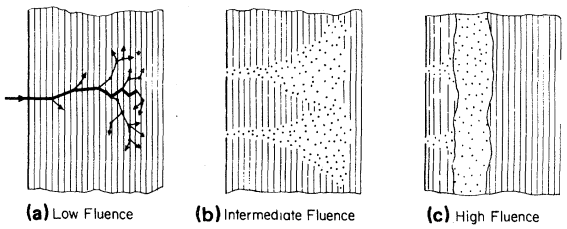

FIG. 1. Schematic view of the disordered region in graphite caused by implantation at (a) low, (b) intermediate, and (c) high fluence.

The Raman spectra of several forms of graphite have been reported by Tuinstra and Koenig.[8] It has been noted that while single-crystal graphite and highly oriented pyrolytic graphite (HOPG) exhibit a sharp Raman line [Fig. 2(a)] at $\sim$ 1580 cm^{-1}, more poorly ordered graphite materials, such as activated charcoal[8] or glassy carbon,[5] exhibit two Raman lines [Fig. 2(b)], one near $\sim$ 1580 cm^{-1} and an additional line near $\sim$ 1355 cm^{-1} where the phonon density of states has a strong maximum. Tuinstra and Keonig[8] have shown that the relative intensity of the disorder-induced 1355-cm^{-1} line relative to the Raman-active 1580-cm^{-1} line, I(1355)/I(1580), varies inversely with the crystallite size L_a of the graphite sample. For thin ($<<$ 2500 Å) amorphous carbon films deposited on glass substrates,[9] the two lines are no longer resolved and a very broad asymmetric Raman line is observed [see Fig. 2(c)]. However, thick carbon films ($\gtrsim$ 2500 Å) deposited on glass exhibit a two-peak Raman spectrum.

Previous studies on ion-implanted graphite[2,6] have yielded the broad line characteristic of the amorphous regime [see Fig. 2(c)]. The first measurements by Crowder *et al.*[2] were made on graphite implanted with ^{40}Ar ions at a fluence of 1×10^{16} ions/cm^2, and the overall study was directed toward an elucidation of the effect of ion implantation on the tetrahedral bonding arrangement in common semiconductors. Crowder *et al.*[2] showed that a similar broad asymmetric Raman line, characteristic of the amorphous regime, was obtained upon ion

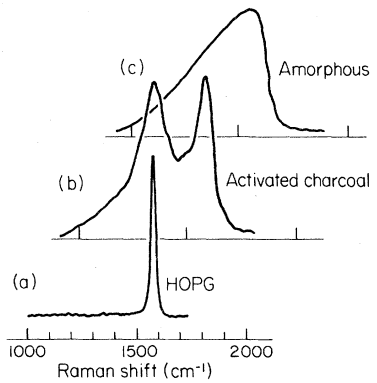

FIG. 2. Experimental Raman spectra from various kinds of graphite. (a) Single-crystal graphite and HOPG with a single line near 1580 cm^{-1}. (b) Activated charcoal showing the Raman-active E_{2g_2} line near 1580 cm^{-1} and a disorder-induced line near 1355 cm^{-1}. (c) A broad asymmetric line from an amorphous film peaked near 1500 cm^{-1} (from Ref. 9).

implantation of either graphite or diamond, showing that ion implantation destroyed the local tetrahedral bonding arrangement of diamond. Later work by Wright *et al.*[6] was carried out on ultra superior purity graphite (USP) samples, showing Raman spectra similar to Fig. 2(b) prior to implantation with 10–15 keV ^{1}H, ^{2}D, and ^{4}He ions and fluences up to 4×10^{19} ions/cm^2. Their first-order Raman spectra also exhibited the broad asymmetric line after implantation [see Fig. 2(c)]. Annealing at 1040 °C for 3 h restored the double-peaked spectra [see Fig. 2(b)] for USP samples that had been implanted with ^{2}D ions at 15 keV to a fluence of 2.7×10^{19} ions/cm^2. A broadening effect of ion implantation on the second-order spectra was also reported by Wright *et al.*[6] Raman spectroscopy has also been used to monitor the effect of fast neutron irradiation at low temperature (5 K) followed by room-temperature annealing,[7] in which the focus was on monitoring the radiation damage of reactor materials.

In the present study, attention is focused on implanted ions with masses comparable to that for the graphite host. A relatively low fluence ($10^{14} \lesssim \phi \lesssim 10^{16}$ ions/cm^2) has been used, which permits us to investigate for the first time the disorder produced by ion implantation prior to the formation of the amorphous layer (see Fig. 1). Results for the effect of annealing on the implanted samples are reported for the range of fluences near the threshold for formation of the amorphous layer. Our measurements of the second-order Raman scattering show the second-order spectra to be even more sensitive than the first-order spectra to monitoring the threshold for formation of the amorphous layer.

EXPERIMENTAL

Samples of highly oriented pyrolytic graphite (HOPG) have been implanted with carbon ions and ions of atomic mass less (^{6}Li, ^{9}Be, ^{11}B)and greater (^{31}P, ^{75}As) than that of carbon. Carbon ions are of special interest because only carbon impurities are introduced during the implantation process, thereby making it possible to distinguish the effects caused by the ion implantation itself from the effects caused by the implantation of ions differing from the host material. An Accelerators Inc. 300*R* ion implanter was used for the implantation and the ion beam was directed normal to the graphite *c* face. The samples were implanted at ambient temperatures, with fluences in the range 1×10^{14} ions/cm^2 to 2.5×10^{16} ions/cm^2, and at an accelerating voltage of 100 keV.

The Raman scattering experiments were performed at room temperature using a Brewster angle backscattering geometry. Incident radiation of 4880 Å and ~200 mW was provided by a cw argon-ion laser. The scattered radiation was collected 90° to the sample surface, analyzed by a double-grating monochromator and detected by a cooled photomultiplier tube.

Repeated Raman spectra showed the ion-implanted samples to be stable with respect to time and ambient laboratory atmosphere. At the low laser powers used in the Raman scattering measurements, no laser annealing effect was expected or observed. The ion-implanted samples were isochronally vacuum annealed in quartz tubes in the temperature range $700 < T < 1000$ °C.

RESULTS AND DISCUSSION

Raman spectra of HOPG implanted with ^{9}Be, ^{11}B, ^{12}C, and ^{31}P at a fixed fluence of 1×10^{14} ions/cm^2 are presented in Fig. 3. These spectra are from unannealed samples and for the case of the ^{9}Be, ^{11}B, and ^{12}C ions correspond to the low-fluence regime (as discussed below). All spectra show the appearance of Raman intensity in the

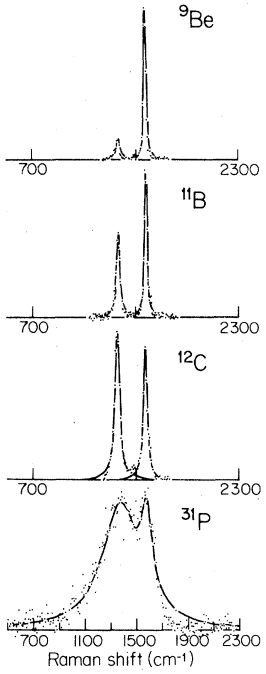

FIG. 3. Room-temperature Raman spectra showing lines at 1355 and 1580 cm^{-1} for unannealed HOPG samples ion implanted with ^{9}Be, ^{11}B, ^{12}C, and ^{31}P at the same fluence, 1×10^{14} ions/cm^2 at 100 keV. The abscissa is linear in wave number and the points are experimental.

vicinity of ~ 1355 cm^{-1}, indicative of disorder-induced scattering.[8,9]

As seen from Fig. 3, the intensity of the 1355-cm^{-1} line relative to that at 1580 cm^{-1} and denoted by $I(1355)/I(1580)$, depends on the atomic mass of the implanted species, the heavier implanted ions giving larger magnitudes for $I(1355)/I(1580)$. The results for atomic masses less than or equal to carbon show well-resolved peaks, in contrast to the behavior for the phosphorus ions ($M = 31$) where the Raman spectrum appears to be qualitatively similar to that for amorphous carbon [Fig. 2(c)]. Expect for the barely resolved doublet structure, the spectrum for the ^{31}P implanted sample at a fluence of 1×10^{14} ions/cm^2 (Fig. 3) is qualitatively similar to that reported by Wright *et al.*[6] for an ^{40}Ar implanted sample at a fluence of 1×10^{16} ions/cm^2. Our results for the Raman spectra of ^{75}As- implanted graphite are qualitatively similar to those for P, indicating a saturation as a function of ion mass and fluence of the intensity ratio $I(1355)/I(1580)$ once the Raman line shape characteristic of amorphous carbon is obtained. For equal incident kinetic energy, the heavier ions are slowed down over a shorter penetration depth, thereby giving rise to a greater density of collision events and a larger cross-sectional damage area per ion. Thus it is reasonable that the transition from the disordered regime [Fig. 1(a)] to the amorphous regime [Fig. 1(c)] occurs at a lower implantation dose as M increases.

As can be seen from Fig. 3, the linewidth of both the 1355- and 1580-cm^{-1} lines increases with increasing atomic mass M of the ions. The increase in linewidth is gradual as M is increased from 9 in Be to 12 in C, in contrast to the dramatic increase in linewidth for the case of phosphorus where $M = 31$.

Insight into the linewidth behavior shown in Fig. 3 is also provided by study of the dependence of the Raman spectra on ion fluence for a single ion species, as shown in Fig. 4(a) for boron ^{11}B ions. This figure shows a gradual increase in relative intensity $I(1355)/I(1580)$ and linewidth of both lines as the fluence in increased from 1×10^{14} ions/cm^2 to 5×10^{14} ions/cm^2 to 1×10^{15} ions/cm^2 . As the fluence of boron is further increased to 5×10^{15} ions/cm^2, a dramatic change in linewidth and intensity occurs and above that fluence the results at 1×10^{16} and 2.5×10^{16} ions/cm^2 show little further change. Results at 1×10^{14} ions/cm^2 and 100 keV for phosphorus (Fig. 3) and arsenic (not shown) appear to be in the same regime of behavior as that which is observed with boron for fluences of 5×10^{15} ions/cm^2 and above. The spectra for samples with high ion concentrations are asymmetric, though two broad lines can be resolved by deconvolution, fitting each component to a Lorentzian line shape. The deconvolution procedure for high ion concentrations, however, results in considerable error in the determination of peak frequencies and linewidths.

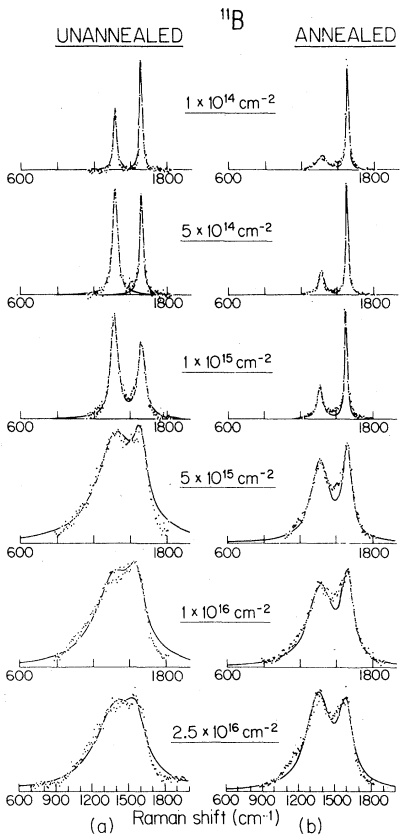

FIG. 4. Raman spectra for various fluences (1×10^{14} to 2.5×10^{16} ions/cm^2) of ^{11}B ions implanted into six HOPG samples. The spectra on the left (a) are for the unannealed samples, and on the right (b) are for the same samples annealed at 950 °C for 0.5 h. The abscissa is linear in wave number and the points are experimental.

Raman spectra are shown in Fig. 4(b) for the same samples that are shown in Fig. 4(a), but after annealing at 950 °C for 0.5 hours. We find that annealing at a temperature as low as 700 °C is sufficient to yield two clearly resolved Raman peaks from samples which have been implanted with ^{11}B ions to fluences in the range $5 \times 10^{15} \lesssim \phi \lesssim 2.5 \times 10^{16}$ ions/cm^2, and had exhibited the broad asymmetric line shape characteristic of the amorphous layer [see Fig. 4(a)]. Thus annealing provides a partial restoration of the structural order of the pristine graphite, consistent with the annealing results obtained by others.[6,9] From studies on Si

and Ge it has been shown that the effect of annealing is more sensitive to the annealing temperature than to the time of annealing, provided that the time is sufficient for the samples to reach thermal equilibrium. Annealing studies of graphite implanted with high fluences of the light ions ^{1}H, ^{2}D, and ^{4}He, however, showed a weak dependence on the annealing time.[6] It is clear from Fig. 4 that for all ion concentrations shown, annealing at 950 °C causes a partial restoration of crystalline order. With regard to the disorder-induced 1355-cm^{-1} line, annealing causes both the intensity and linewidth to decrease . For the Raman-active 1580-cm^{-1} line, annealing causes an increase in intensity and a decrease in linewidth. For both unannealed and annealed samples the line shapes for fluences $\phi \geq 5 \times 10^{15}$ ions/cm^2 are qualitatively different from the behavior below this fluence. In these spectra no evidence for carbide formation in terms of carbide-specific Raman lines was found for our experimental conditions. The absence of such lines may be due to the low annealing temperatures or the relatively low implanted-ion concentrations used in these experiments.

A summary of results for the first-order Raman spectra is given in Figs. 5 and 6, where the linewidths (FWHM) of the 1355- and 1580-cm^{-1} lines are, respectively, plotted as a function of $\log_{10}\phi$, where ϕ is the boron fluence. Also plotted on this figure are the results obtained after annealing at two different temperatures. The linewidths are determined by fitting the experimental data to a Lorentzian line shape. Figure 5 dramatically shows

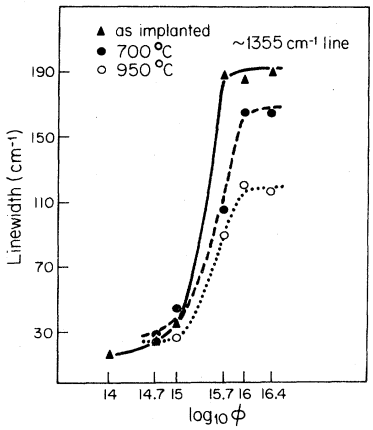

FIG. 5. Graph of the 1355-cm^{-1} linewidth (FWHM) versus $\log_{10}\phi$ for ^{11}B ion implanted HOPG, where ϕ is the boron fluence. Results are presented for unannealed samples and for the same samples annealed at 700 °C and 950 °C.

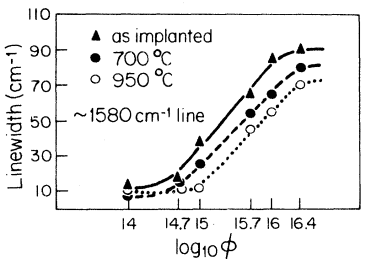

FIG. 6. Graph of the 1580-cm^{-1} linewidth (FWHM) versus $\log_{10}\phi$ for ^{11}B ion implanted HOPG where ϕ is the boron fluence. Results are presented for unannealed samples and for the same samples annealed at 700 °C and 950 °C.

the rapid change in linewidth of the 1355-cm^{-1} line in the vicinity of a fluence of $\phi \gtrsim 1 \times 10^{15}$ ions/cm^2. The linewidth changes with annealing are very small for $\phi \leq 1 \times 10^{15}$ boron ions/cm^2 and are very significant above this fluence, though the fluence range over which the change in linewidth in Fig. 5 occurs is not sensitive to annealing for annealing temperatures $\lesssim$ 950 °C. Noting that the Raman-active 1580-cm^{-1} line is much narrower than the disorder-induced 1355-cm^{-1} line at low fluences, the order-of-magnitude increase in linewidth from low to high boron-ion fluence is of comparable size for both the 1355-cm^{-1} and 1580-cm^{-1} lines. However, the fluence range over which this increase in linewidth occurs is larger for the 1580-cm^{-1} line than for the 1355 line. The percent reduction in linewidth due to annealing is larger for the 1355-cm^{-1} line than for the 1580-cm^{-1} line.

In connection with the linewidths of the first-order spectra, it is of interest to note that the introduction of guest species by chemical intercalation does not significantly increase the linewidths of the first-order Raman spectra,[10] even for the lowest-stage compounds (i.e., highest intercalate concentration), indicating that intercalation does not radically reduce the in-plane graphite crystallite size. The anomalous broadening of the first-order Raman spectra for the stage 1 alkali metal compounds is attributed to a strong coupling between the discrete E_{2g_2} mode and a continuum of phonon states, and not to a reduction in the in-plane graphite crystallite size.[11] On the other hand, the E_{2g_2} mode frequency is known to vary with intercalation, being upshifted linearly as a function of reciprocal stage $(1/n)$ for acceptor intercalants and downshifted for donor intercalants.[12] It is also well known[13] that the disordering of the graphite lattice upshifts the first-order Raman E_{2g_2} mode frequency, with a sensitivity to crystallite size that depends on the ra-

quency (up to 12 cm^{-1}) with decreasing crystallite size is suggested to be a consequence of both a breakdown in the wave-vector selection rule and a phonon dispersion branch that rises away from the zone center, thereby admixing phonons with both larger wave vectors and higher frequencies.

These considerations inspired investigation of the behavior of the frequency shift of the 1580-cm^{-1} line relative to that for HOPG and the results are shown in Fig. 7 for samples implanted with boron. A dramatic change in the mode frequency shift $(\nu - \nu^{HOPG})$ is found for fluences ϕ in the range where the linewidth changes rapidly. This behavior suggests that at low fluence there is an upshift of the E_{2g_2} mode, consistent with the increasing disorder [Fig. 1(a)] and formation of microcrystallites [Fig. 1(b)]. At high fluence, where the structure becomes amorphous, the downshift of the E_{2g_2} mode might be associated with an expansion of the C—C in-plane distance, similar to the effect observed in donor graphite intercalation compounds.[12,14,15] The behavior of the annealing data in Fig. 7 is particularly intersting and may upon detailed examination yield information on activation energies for the transition of an ion from an interstitial to a substitutional site.

Second-order (two phonon) Raman spectra have been reported for various types of graphite samples, exhibiting a variety of crystallite sizes.[13] The dominant feature in the second-order spectrum is an intense line at 2735 cm^{-1}. A very sharp but weak feature at 3248 cm^{-1} and a feature at 2970 cm^{-1} which is caused by lattice disorder, have also been reported.[13] Nemanich *et al.* show that the feature at ~2735 cm^{-1} becomes broader, the one at ~2970 cm^{-1} becomes more intense, and the one at 3248 cm^{-1} is suppressed with decreasing crystallite size.[13] In contrast, the second-order Raman spectra for single-crystal graphite and HOPG show no structure at 2970 cm^{-1} and a partially-resolved doublet structure at 2735 cm^{-1}.[13,16,17] Our measurements on HOPG show additional sharp features in the second-order spectra at 2327 cm^{-1}, 2435 cm^{-1}, and a broader feature at 2468 cm^{-1} (see Fig. 8). Wright *et al.*[6] have also reported a broad feature at 2445 cm^{-1} in USP graphite, corresponding to the doublet structure in Fig. 8 at 2435 cm^{-1} and 2468 cm^{-1}. This feature is also evident in the second-order spectra for HOPG shown in Ref. 17. The sharp feature at 2327 cm^{-1}, reported here for the first time, was observed using laser excitation wavelengths of 4880 and 5145 Å.

Previous workers have identified the 2970-cm^{-1} feature in the second-order spectra with disorder-induced scattering, analogous to the 1355-cm^{-1} line in the first-order Raman spectra.[6,13,16,17] The identification of this feature in the second-order spectra can be made using the density of phonon states[18] calculated on the basis of the graphite phonon dispersion relations of Maeda *et al.*[19] The main peaks in the phonon density of states occur at 1620, 1360, 850, 830, and 570 cm^{-1}. Thus 2(1620) cm^{-1} = 3240 cm^{-1} and 2(1360) cm^{-1} = 2720 cm^{-1} correspond, respectively, to the peaks at 3248 and 2730 cm^{-1} in the second-order Raman spectra. The disorder-induced peak at 2970 cm^{-1} corresponds to (1620 + 1360) cm^{-1} = 2980 cm^{-1} and therefore involves two phonons at somewhat different points in the Brillouin zone, consistent with a disorder-induced mechanism. We also note that the doublet structure in the density of states at 830 and 850 cm^{-1} combines with the 1620-cm^{-1} peak to

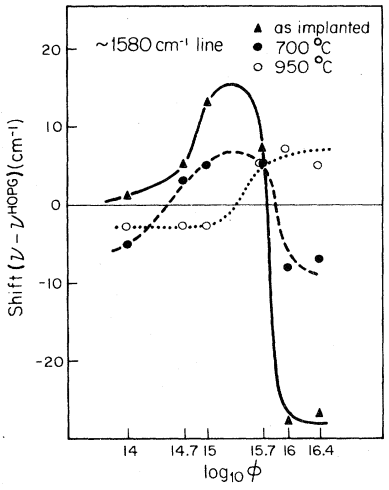

FIG. 7. Graph of the frequency shift of the 1580-cm^{-1} line with respect to that of unimplanted HOPG versus $\log_{10}$ of the boron fluence ϕ. Results are given for both the unannealed samples and for the same samples annealed at 700 and 950 °C.

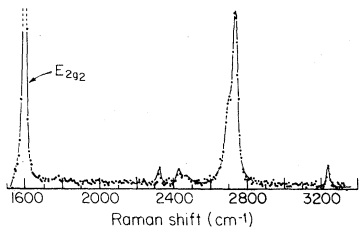

FIG. 8. Second-order Raman spectra of HOPG. An intense line occurs at 2735 cm^{-1} and a very sharp feature at 3248 cm^{-1}.

yield 2450 and 2470 cm^{-1}, which are close to the observed peaks in the second-order Raman spectra at 2435 and 2468 cm^{-1}. No identification has been made of the sharp feature in the second-order spectrum at 2327 cm^{-1}.

Results for the second-order Raman spectra from HOPG samples implanted with various fluences of 100-keV boron ions are given in Fig. 9(a). These spectra also show a strong dependence on boron fluence, with results analogous to the first-order spectra for the ion-implanted samples. However, in the case of the second-order spectra, additional interesting phenomena are observed with increasing concentration of implanted ions. As boron ions are introduced, a feature at 2970 cm^{-1} appears, and its intensity is increased with increasing boron-ion dosage up through a fluence of 5×10^{14} ions/cm^2. For a fluence of 1×10^{15} ions/cm^2, the 2970-cm^{-1} feature becomes broadened and shows a decrease in peak intensity. At fluences of 5×10^{15} ions/cm^2 and above, the feature at 2970 cm^{-1} cannot be resolved form the broad background. In comparison to second-order spectra previously reported for samples with various crystallite sizes,[13] the results in Fig. 9(a) indicates that the effect of implantation of 100-keV boron ions is the introduction of disorder and reduction of the ordered crystallite size. We may identify the onset of amorphous behavior with the disappearance of the second-order spectral features. Second-order Raman spectra have previously been reported by Wright *et al.* for 4.1×10^{19} ^1H ions/cm^2 at 15 keV showing a very broad band, peaking at 2890 cm^{-1}, and a weaker broad feature at 2150 cm^{-1}, not found in graphite and identified with the occurrence of conjugated acetylenic bonds.[6]. We note that a combination of two peaks in the phonon density of states (1620 + 570) cm^{-1} = 2190 cm^{-1}, which suggests a disorder-induced second-order feature analogous to the feature at 2970 cm^{-1}.

As shown in Fig. 9(b) the effect of annealing in this case is even more dramatic than for the first-order spectra. For fluences of 5×10^{14} ions/cm^2 and below, annealing at a temperature as low as 700 °C sharpens the 2730 cm^{-1} line and reduces the intensity of the 2970 cm^{-1} feature, indicating some restoration of order by the annealing process. For the sample that had been implanted at 10^{15} ions/cm^2, this low-temperature (700 °C) anneal restored the second-order Raman spectra to an extent corresponding approximately to that for the 5×10^{14} ions/cm^2 unannealed sample. However, for fluences of 5×10^{15} ions/cm^2 and above, annealing at 700 °C (or at temperatures up to 1000 °C) did not restore any of the features in the second-order spectra. From comparison of Figs. 4 and 9 we suggest that the second-order lines are much more sensitive to the restoration of order by annealing than the first-order lines.

Results for the first- and second-order Raman spectra for graphite implanted with boron ions indicate three regimes of behavior. At low fluence ($\phi \leq 5 \times 10^{14}$ ions/cm^2), the first- and second-order Raman spectra show relatively sharp features which we identify with an ordered sample containing pockets of disorder caused by ion implantation. At a fluence of $\sim 1 \times 10^{15}$ ions/cm^2, the first-order spectrum starts to broaden while the second-order spectrum becomes greatly attenuated, although it is partly restored by annealing. We suggest that at a fluence of 1×10^{15} ions/cm^2, the regions of disorder (see Fig. 1) begin to coalesce (percolate), forming islands of ordered regions surrounded by disorder. This may be called the microcrystalline regime. At this fluence level, annealing has the most significant effect on the first- and second-order spectra, consistent with the restoration of sufficient order

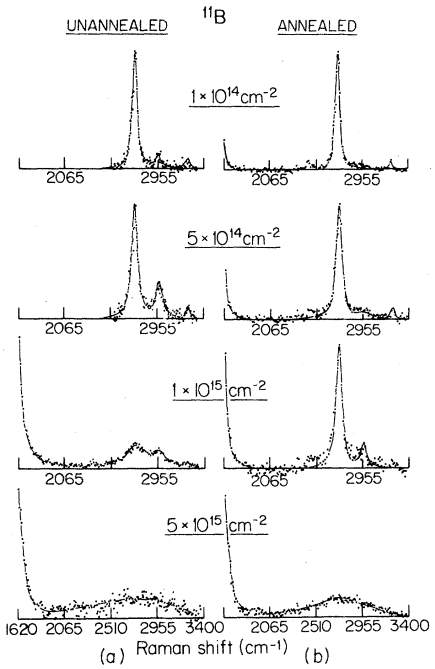

FIG. 9. Room-temperature second-order Raman spectra for various fluences (1×10^{14} to 5×10^{15} ions/cm^2) of ^{11}B ions implanted into four HOPG samples. Results are given for the unannealed samples (a) and for the same samples annealed at 700 °C for 0.5 h (b).

to inhibit the coalescence of the disordered regions. At higher fluences where the coalescence of the disordered regions is well established, the microcrystalline regions shrink in size, and annealing is ineffective in inhibiting the coalescence of the disordered regions. This may be called the amorphous regime.

Work is in progress to explore the behavior of the electrical conductivity in these three regimes of ion fluence and to correlate the behavior of the electrical conductivity with the Raman spectra reported here.

ACKNOWLEDGMENTS

We are thankful to Dr. Yasuo Wada of Hitachi Research Laboratory and Nobuyuki Kambe of M.I.T. for their collaboration in the early phases of this research. We thank Mark Rothman of M.I.T. for technical assistance and Dr. A. Moore of Union Carbide for the HOPG material. We also express our gratitude to R. Al-Jishi for discussions and to ONR Grant No. N00014-77-C-0053 for supporting this research.

[1]J. W. Mayer, L. Eriksson, and J.A. Davis, *Ion Implantation in Semiconductors* (Academic, New York, 1970).

[2]B. L. Crowder, J. E. Smith, Jr., M. H. Brodsky, and M. I. Nathan, *Proceedings of the Second International Conference on Ion Implantation in Semiconductors* (Garmisch-Partenkirchen, Federal Republic of Germany, 1970), p.255; J. E. Smith, Jr., M. H. Brodsky, B. L. Crowder and M. I. Nathan, J. Non-Cryst. Solids 8—10, 179 (1972).

[3]R. Beserman and T. Bernstein, J. Appl. Phys. 48, 1548 (1977).

[4]Herbert Engstrom and J. B. Bates, J. Appl. Phys. 50, 2921 (1979).

[5]M. I. Nathan, J. E. Smith, Jr., and K. N. Tu, J. Appl. Phys. 45, 2370 (1974).

[6]R. B. Wright, R. Varma, and D. M. Gruen, J. Nucl. Mater. 63, 415 (1976).

[7]H. Maeta and Y. Sato, Solid State Commun. 23, 23 (1977).

[8]F. Tuinstra and J. L. Koenig, J. Chem. Phys. 53, 1126 (1970).

[9]S. A. Solin and R. J. Kobliska, *Proceeding of the 5th International Conference on Amorphous and Liquid Semiconductors* (Taylor and Francis, London, 1974), p. 1251; N. Wada, P. J. Gaczi, and S. A. Solin, J. Non-Cryst. Solids 35 and 36, 543 (1980).

[10]M. S. Dresselhaus and G. Dresselhaus, in *Physics and Chemistry of Materials with Layered Structures,* edited by F. Lévy (Reidel, Dordrecht, Holland, 1979), Vol. 6, p. 423; M. S. Dresselhaus and G. Dresselhaus in *Light Scattering in Solids,* edited by L. Cardona and G. Güntherodt (Springer, Berlin, 1981) (in press).

[11]P. C. Eklund, G. Dresselhaus, M. S. Dresselhaus, and J. E. Fischer, Phys. Rev. B 16, 3330 (1977); P. C. Eklund and K. R. Subbaswamy, *ibid.* 20, 5157 (1979).

[12]S. Y. Leung, G. Dresselhaus, and M. S. Dresselhaus, Synth. Met. 2, 89 (1980).

[13]R. J. Nemanich, G. Lucovsky, and S. A. Solin, Mater. Sci. Eng. 31, 157 (1977).

[14]D. E. Nixon and G. S. Parry, J. Phys. C 2, 1732 (1969).

[15]S. A. Solin, Mater. Sci. Eng. 31, 153 (1977).

[16]R. J. Nemanich and S. A. Solin, Phys. Rev. B 20, 392 (1979).

[17]P. C. Eklund, D. S. Smith, V. R. K. Murthy, and S. Y. Leung, Synth. Met. 2, 99 (1980).

[18]S. Y. Leung, M. S. Dresselhaus, and G. Dresselhaus, Physica (in press).

[19]M. Maeda, Y. Kuramoto, and C. Horie, J. Phys. Soc. Jpn. 47, 337 (1979).